A comparison of the performance of four acoustic modulation techniques for robot communication in pipes

Zhengwei Li, Yicheng Yu, Kirill V. Horoshenkov*

Department of Mechanical Engineering, University of Sheffield, Mappin Street, Sheffield S1 3JD, United Kingdom

*Corresponding author. Email: k.horoshenkov@sheffield.ac.uk Tel. +44 7776160235

Keywords: in-pipe acoustic communication, acoustic channel characterisation, package error rate, deconvolution

ABSTRACT

Autonomous robotics is an emerging technology for the inspection of a vast network of underground pipes. Communication between autonomous robots is essential to optimise their efficiency and network coverage. However, sending message acoustically is not a well-researched topic because most of the existing literature is devoted to the study of the acoustic properties of the pipe for the purpose of sensing rather than communication. In particular, the influence of multi-modal propagation and background noise on the quality of acoustic communication in pipes has not been well understood. This paper studies the performance of four standard acoustic communication techniques in a dry drainage pipe to fill this knowledge gap. The noise resistance, communication range and data rate of these techniques are estimated through numerical simulations and laboratory experiments. It has been found that the techniques based on shift keying requires at least 5-10 dB signal to noise ratio (SNR) to function properly while the chirp linear frequency modulation technique can operate reliably with SNR = 0 dB or event lower SNR. The results also suggest that the multi-modal propagation in the pipe has significant effects on the package error rate. The frequency dependent sound attenuation in the pipe also affects the communication range and data rate. In particular, for a 150 mm diameter dry pipe the maximum robot operation distance is likely to be limited to 50-100 m with the highest carrier frequency of around 10 kHz and data rates below 6300 bps. The results of this work pave the way to the development of acoustic communication modules to be deployed on tetheless robots designed to inspect a buried pipe network autonomously and collaboratively.

1. Introduction

There are millions of kilometres of buried wastewater collection pipes around the globe. A considerable proportion of this system is ageing and failing resulting in blockages, pollution spills and flooding in urban areas. Real time condition data to prevent these failures proactively are rare and repair and rehabilitation of these assets are generally reactive via disruptive excavation. In order to address this problem, the British government invested heavily to develop the science of miniature, cooperating swarms of autonomous robots for the inspection of buried pipes [1]. The focus of the Pipebots team is on new science which is emerging from the latest advances in robotics, sensing, control, additive manufacturing and artificial intelligence (AI). Findings from the Pipebots project suggests that that the success of autonomous robotic sensing in a very large pipe network depends on the ability of these robots to communicate information on the position and local conditions wirelessly [2]. Robust communication in a robot swarm is essential to achieve good performance for a robotic swarm inspecting autonomously a large, buried pipe network.

It is common to use radio waves (FR) to communicate messages above ground. However, this is problematic in buried sewer pipes because the RF attenuation is too high. In a pressurized water pipe, optical waves have desirable advantage in terms of high data rate reaching Gbps. However, it only works as a line-of-sight communication and in the absence of scatterers such as fog, spray and dust. In this respect acoustic waves are attractive to use for communication, because they propagate relatively long distances with little attenuation [3]. In addition, relatively low cost, simple and robust acoustic sensors are more suitable to work in the harsh environment such as sewer pipes to deliver messages between robots and for being used for detecting a critical change.

To the best of our knowledge there have been very few studies into the in-pipe acoustic communication. In 1997, Li et al [4] used simulation-based approach to develop an underwater ultrasonic acoustic communication system for water tanks and pipes to study the effects of multipath propagation. This work is relevant as it reflects the challenges of sending messages acoustically in the pipe, but it is restricted to ultrasound. The authors pointed out that the effect of multi-modal propagation in a pipe will be much stronger than multi-path propagation in a tank which requires efficient equalisation techniques and choosing modulation method wisely to overcome those effects. However, his work only presents the existing challenges and there was no demonstration of a successful in-pipe acoustic communication. The details of communication such as encoding and MODEM (Modulation & Demodulation) were also not mentioned in this paper. In 2000, Kokossalakis [5] has discussed the basic process of deploying acoustic wireless sensor networks to transmit data in multi-shape, air-filled pipe which illustrates the physical acoustics of a duct and method of encoding and decoding, MODEM and equalisation. His work elaborated on most of the details that need to be considered for in-pipe acoustic communication, and the simulation results were successfully verified by experiments. Unfortunately, from a realistic perspective, the reliability of the communication system yes needs to be tested and challenged via different parameters such as noise resistance, communication range and data rate, which were exactly what this work lacks. Jing et al [6] used analytical and experimental method to determine a 1-50 kHz wideband acoustic channel characterisation of straight gas and oil pipe. Their work reflects the importance of predicting and measuring the frequency response function (FRF) of the pipe for acoustic communication. In their another study in 2020 they developed an encoding method of Orthogonal Frequency Division Multiplexing (OFDM) for low and high SNR situations in a water filled pipe [7]. In 2021 Yu et al [8] utilised analytical, numerical, COMSOL and FEM methods for channel characterisation of partially water filled pipe. The works by Jing [6] and Yu [8] papers suggest that the channel properties of a realistic pipe with different conditions could be predicted by non-experimental approaches which are accurate to support the further simulation-based study of in-pipe acoustic communication and in this case, the difficulty of getting access to the pipe will be minimised accordingly.

There is still a lack of data on the effects of muti-modal sound propagation in a pipe, background noise and attenuation on the package error rate observed when using popular acoustic communication technologies. This information is essential to design communication solutions that can be adopted on a moving robot working autonomously in a pipe. This paper attempt to address the existing gaps in knowledge by studying the performance of four acoustic communication techniques in a dry drainage pipe and influence of the SNR and cut-off frequencies on the package error rate. The novelty of this work is in a systematic study how classic acoustic communication techniques perform in a multi-modal pipe environment in the presence of noise and attenuation. This work is based on a validated analytical approach to predict the FRF of the channel which is then experimentally tested. It demonstrates the importance of the deconvolution to equalise the effects of multi-mode propagation and noise.

The four communication techniques studied here are based on amplitude, phase and frequency shift keying, and chirp linear frequency modulation [9]. The performance of each of these four communication techniques is evaluated in terms of its package error rate, noise resistance, communication range and maximum data speed. Factors which affect the data speed for these four communication techniques are analysed and discussed.

The paper is organised in the following manner. Section 2 presents the theory for sound propagation in air-filled pipes which is used for channel characterisation through simulation. Section 3 uses binary amplitude shift keying modulation (2ASK) as an example to demonstrate the procedures of communication in the MATLAB-based simulation. Then section 4 describes the fundamental theories of three binary modulation techniques and chirp linear frequency modulation (CLFM). Finally, the results of simulations and experimental validation are discussed in section 5. In addition, this section also suggested the communication range and maximum data rate for each technique that can be affected by sound attenuation in the pipe.

2. Channel Characterisation

2.1 Theory

In any type of communication technique which relies on acoustic wave propagation, e.g. underwater, channel characterisation is essential because it expresses the physical environment for waves to transmit the signal. For in-pipe communication, the channel is the response of the pipe to an acoustic stimulus. The structure of a real pipe can be complicated by junctions, lateral connections, changing water level, varying cross-section and occasional blockages. These properties of the channel can change over time and sound propagation through it needs to be predicted with a numerical model, e.g. [8]. Such communication channel is usually called 'time-varying channel'.

It makes sense to start with a simpler problem, i.e., with a dry, clean, uniform and infinitely long pipe. It also makes sense to assume that the pipe is filled with air and that its walls are rigid. In this case, the channel is parametrically stabilised. The parametrically stabilised channel is a linear network which means if the transmitting properties are determined, the influence of the channel can be obtained by applying the linear analysis approach. Generally, transmitting properties are expressed by 'amplitude-frequency relations' and 'phase-frequency relations'. However, in a real pipe it is very hard to achieve the ideal condition for both properties and directly transmitting message in such channel would possibly to be under risk of being distorted. Therefore, obtaining and understanding the acoustic channel properties in advanced and applying linear equalisation techniques is essential for the success of in-pipe acoustic communication.

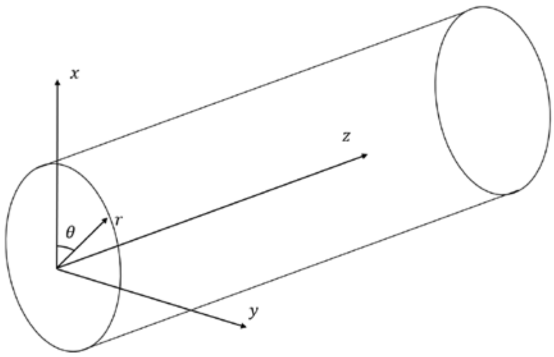

Figure 1.The geometry of the problem of sound propagation in a pipe.

Figure 1 illustrates the cylindrical coordinates system that describes the geometry corresponding to a typical pipe. In these coordinates the frequency-dependent sound pressure can be expressed as the function of the coordinates r, θ and z. The frequency response function (FRF) in these coordinates can be written as:

$$\frac{p(\omega)}{Q(\omega)} = \frac{\omega\rho_0}{\pi R^2}\sum_{m=0}^{\infty}\sum_{n=0}^{\infty}\frac{J_m(k_{mn}r_s)\cos m\theta\left[J_m(k_{mn}r)e^{j|z|\gamma_{mn}}\right]}{(\delta_{m0}+1)\gamma_{mn}J_m^2(k_{mn}R)\left[1-\left(\frac{m}{k_{mn}R}\right)^2\right]} \quad (1)$$

The total process of deriving the above FRF can be found in our previous work [8]. Eq. (1) demonstrates the FRF as the relation between the sound pressure p at (r,θ,z) and the input point source at $(r_s,0,0)$ with volume velocity Q . m and n are mode indices, $j=\sqrt{-1}$, $J_m(k_{mn}r)$ is the m^{th} order Bessel function and A_{mn} is the amplitude of the modes for sound pressure that depend on the source position only. k_{mn} is modal wavenumber, $\gamma_{mn} = \sqrt{k^2-k_{mn}^2}$ is the wavenumber in z direction and k is wavenumber in free space. The cos represents the radial lines of zero pressure which is so called nodal surfaces that occur at angular intervals of π/m and circumferential particle velocity component is maximum at these surfaces. In addition, R is radius of the pipe, ρ_0 is density of air and δ_{m0} is Dirac function.

The equation above predicts the acoustic FRF of the pipe due to a monopole source. It is clear that phase, amplitude and sound velocity in these modes are frequency-dependent and sound propagation in the pipe is multi-modal, i.e. there is a plurality of paths in which sound emitted by the source can reach the receiver. When the frequency of sound passes the so-called cut-off frequency, i.e. $k_{mn} = k$, the phase velocity for the sound waves in the mode (m, n) is infinite and considerable stretching of a sound waveform can occur. Such effect can have a strong influence on the channel communication quality.

2.2 Experimental validation

In order to validate the theory used to predict sound propagation in a pipe an experiment was carried out in a 150mm diameter, 15m long, rigid wall PVC pipe. This setup is shown schematically in Figure 2.

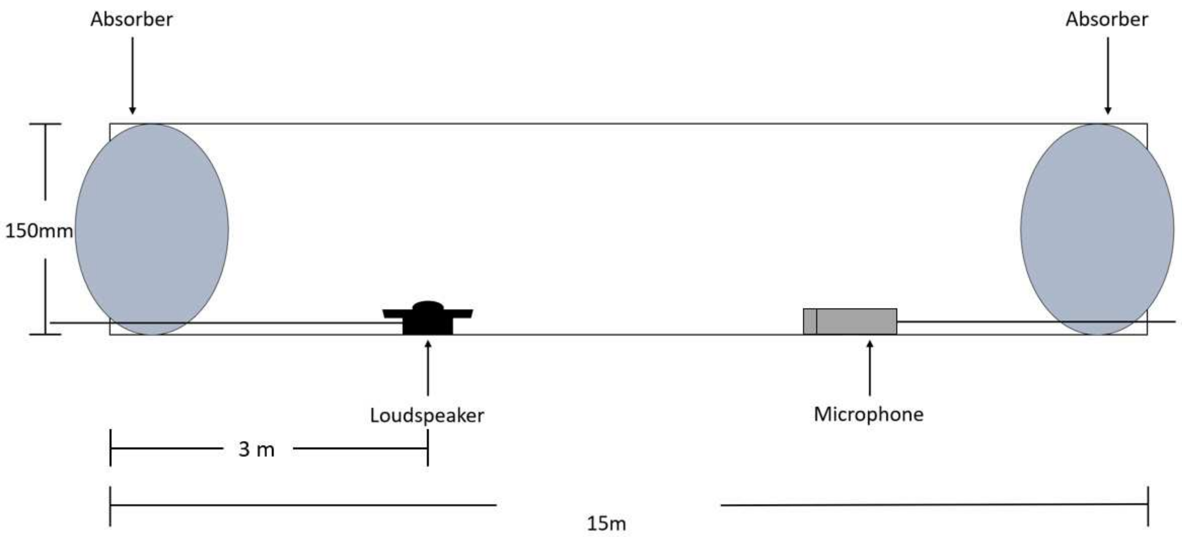

Figure 2. Experiment setup for channel measurement.

On both sides of the pipe, two foam absorbers were inserted to control the reflections caused by the open ends. Then, a 32 mm diameter loudspeaker was placed on the bottom of the pipe 3 m away from the left end of the pipe and faced up to ensure both anti-axisymmetric and axisymmetric modes can be successfully excited. The information of these modes can be found from our previous work in [8]. In addition, a 12 mm diameter microphone (Type 46AE GRAS) was placed in line with the loudspeaker to capture the signal. In measurements, the source was fixed at 3 m away from the left side pipe end and the distance between loudspeaker and microphone varied in the range between 20 mm and 7 m with step spacing of 20 mm. The data was collected by the National Instrument DAQ NI PXIE-6358 data acquisition card and whole process was controlled by a LabVIEW based subroutine with sampling frequency of 48 kHz. The dispersion relation was obtained by measuring the impulse response of the channel. In this experiment, a 10 s long sinusoid-sweep with the frequency in the range between 100 Hz and 5000 Hz was excited and deconvolved with recorded signal to determine the impulse response. This approach enabled us to achieve a relatively good signal-noise ratio of around 40 dB but and was used subsequently for the synchronisation in the communication system (see section 3, Communication Procedures).

This experiment has validated in our work [8] that using analytical approach could obtaine the FRF of the pipe which has very close agreement with experimentally measured FRF, expecially for the first 6 modes. Therefore it makes sense to use analytical method to study channel properties for in-pipe acoustic communicaiton from the prospective of reduce the time consumption.

3. Communication Procedures

Messages which are communicated acoustically are usually digitized and coded using a range of modulation techniques. In this paper three binary modulation techniques were used: 2ASK, 2PSK and 2FSK (Amplitude/Phase/Frequency Shift Keying) [11]. These stand for the amplitude, phase and frequency modulation, respectively. Also, a widely used underwater communication technique, Chirp Linear Frequency Modulation (C-LFM) [9] was adopted and modified to suit the in-pipe environment. These four techniques are based on several common procedures illustrated in Figure 3. The performance of these four modulation techniques for communicating messages in a pipe was studied through the channel characterisation. The channel characterisation was carried out via a MATLAB-based simulation and experiment. In this section, only the procedures of numerical study will be specified, and the simulation results will be compared and validated by experimental approach in section 5. Examples of the signals obtained with the model and from the experiment can be found as supplementary data via the link provided in the Appendix.

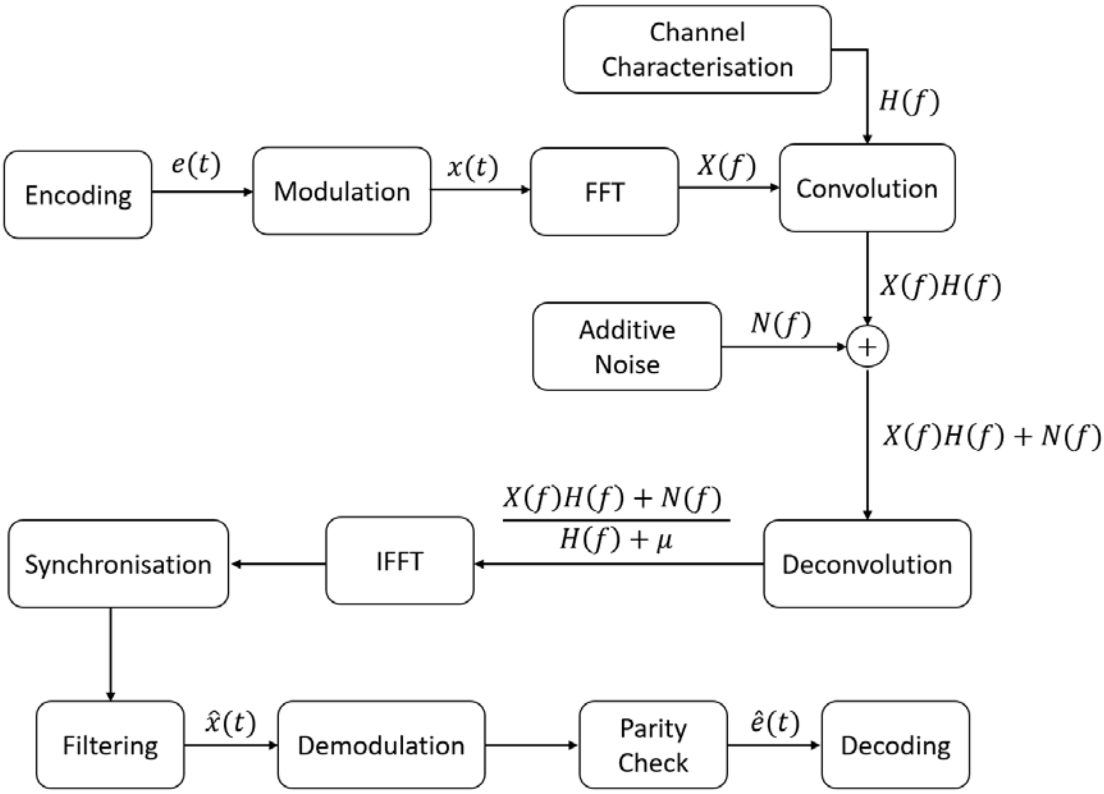

Figure 3 In-pipe acoustic communication simulations procedures

In this simulation, the signal was encoded as 19 binaries which is consisted of 15 random message codes and the 4 ‘ones’ parity checking codes – two at the start and two at the end of the message. The mapping of the message is shown in Table I. In this study the 15 binaries were constantly set as 11101010100011 which is binary form of a random number 25431. It is usual to modulate one of the parameters of the sinusoidal carrier wave (e.g. frequency, phase or amplitude) with these encoded binaries.

1	1	15 random binaries	1	1

Table 1 19 binary message pack

Figure 4 (a) illustrates an example of the signal to broadcast a message using the binary Amplitude Shift Keying (2ASK) modulation technique.

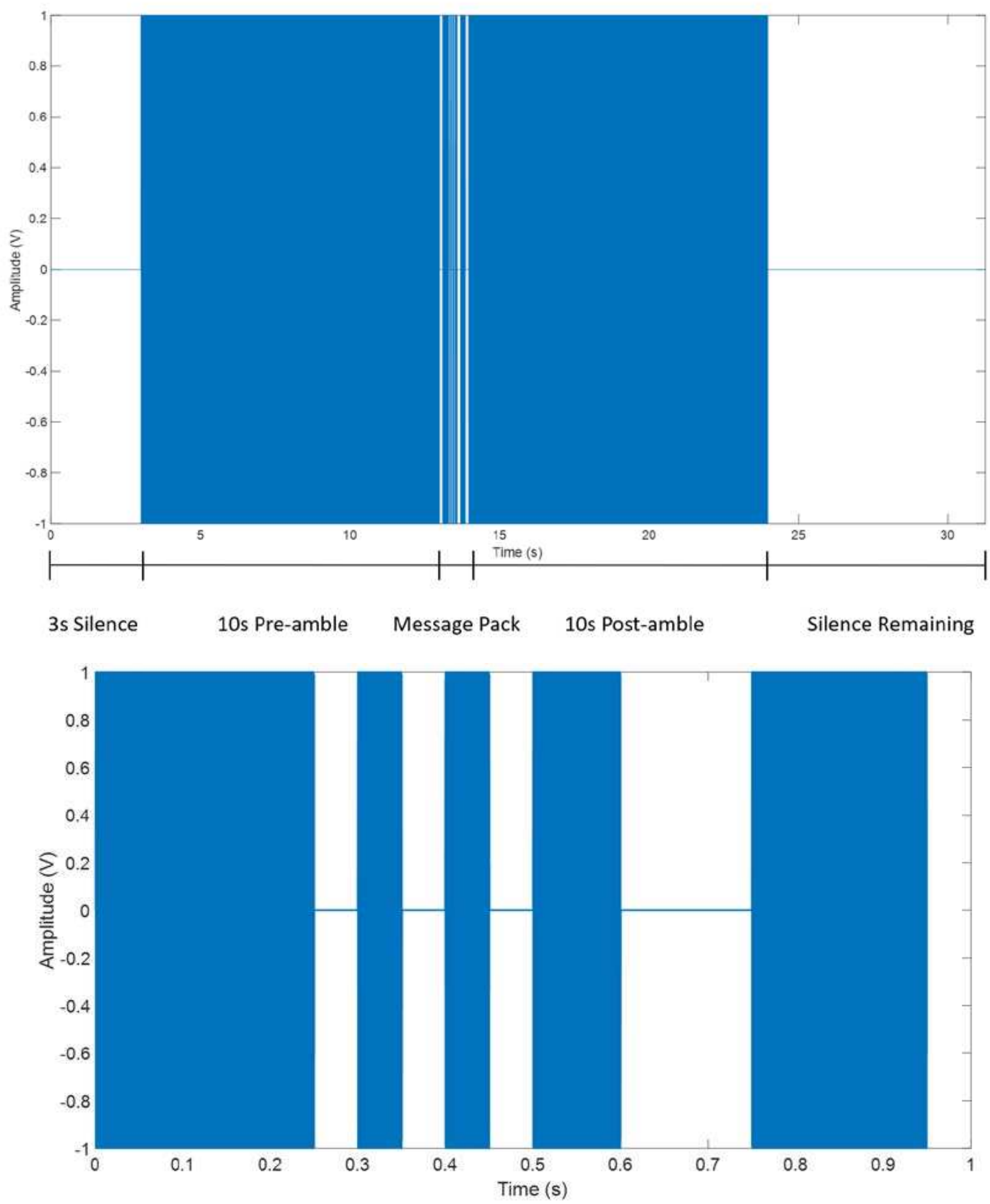

Figure 4. (a) 2ASK signal excitation in time domain (Top). (b) Message package of the signal illustrated in top diagram (Bottom)

This 2ASK signal starts with a 10 s long sinusoid chirp pre-amble with frequency range of 100 Hz - 6000 Hz which signifies the beginning of the communication, after that a 0.1 s interval broadcast and message pack (shown in Figure 4 (b)) is right on the back of the chirp. At the end of the message pack a 0.1 s interval is added followed by an identical chip that works as the post-amble to denote the end of communication. The pre-amble and post-amble can also be used to measure the channel frequency and impulse responses.

The frequency and impulse responses of the pipe measured by the pre- and post-amble is the key to study the influence of channel properties on the modulation signal. In the analysis of linear time-invariant systems the convolution is the most commonly used method to understand the influence of the channel response on the signal. In Figure 3 the encoded signal $e(t)$ will be modulated as $x(t)$ and the process of passing though the channel can be treated as it was convolved with the channel impulse response, $h(t)$. This process is written in the time domain as:

$$g(t) = \int_{-\infty}^{+\infty} x(\tau)h(t-\tau)d\tau \tag{3}$$

In the frequency domain Eq. (3) becomes:

$$G(f) = X(f)H(f) \tag{4}$$

where the capital letters denote the spectra. Usually, background, signal processing and electronic noise $N(f)$ is added to $G(f)$ to simulate the typical channel conditions which are rarely noise free. In this work the noise was only added around the carrier frequency for the 2AKS,2PSK and 2FSK techniques which operate in a narrow band. In the case of the C-LFM technique broadband noise covering the whole frequency range of the chirps was added. The details of modulation will be introduced in the section 'Modulation & Demodulation'. The bandwidth of the noise was determined by $\frac{f_b}{K}$, where f_b is bandwidth of modulation signal and K is the number of binaries in message pack. According to the definition of Signal to Noise Ratio, $SNR = 20\log_{10}\frac{|S(f)|}{|N(f)|}$, where the ratio $\frac{|S(f)|}{|N(f)|}$ is the ratio of signal to noise spectral amplitudes as a function of the frequency f. The noise $N(f)$ can be generated as a random sequence with the spectral amplitude of:

$$N(f) = \frac{1}{A_{RMS}e^{j\phi(f)}10^{\frac{SNR}{20}}} \tag{5}$$

where A_{RMS} is the root-mean square value of the signal spectrum and $\phi(f)$ is random, frequency dependent phase uniformly distributed between $[-\pi, \pi]$.

In order to let the reader have a clearer view on the process of simulation and importance of deconvolution, Figure 5 (a) shows an example of the spectrum of the 20 Hz bandwidth, 5000 Hz carrier frequency 2ASK signal with a 100 Hz - 6000 Hz pre- and post-amble. Figure 5 (b) is the signal propagated through the pipe and predicted 4 m away from the source. Figure 5 (b) also presents the noise spectrum (red line) added to the signal convolution spectrum to study the performance of the communication technique in the presence of background noise. The thick red line denotes the noise level at 0 dB with respect to the root mean square amplitude of the communicated signal. In this example, the bandwidth of the noise covers 80% energy distribution of the modulated signal.

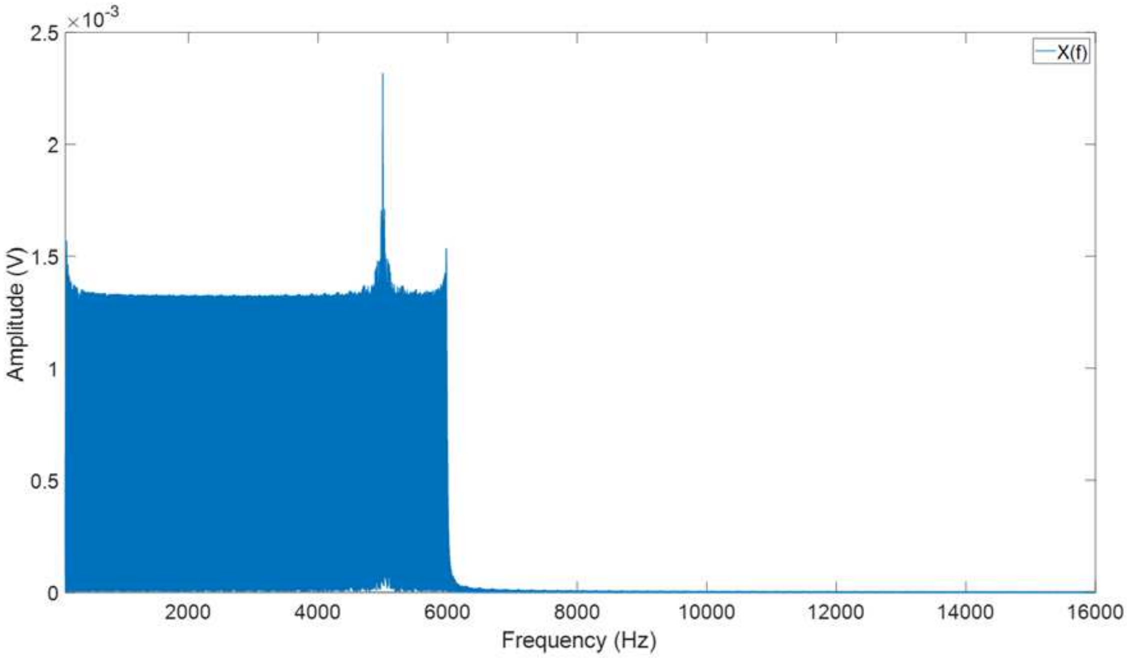

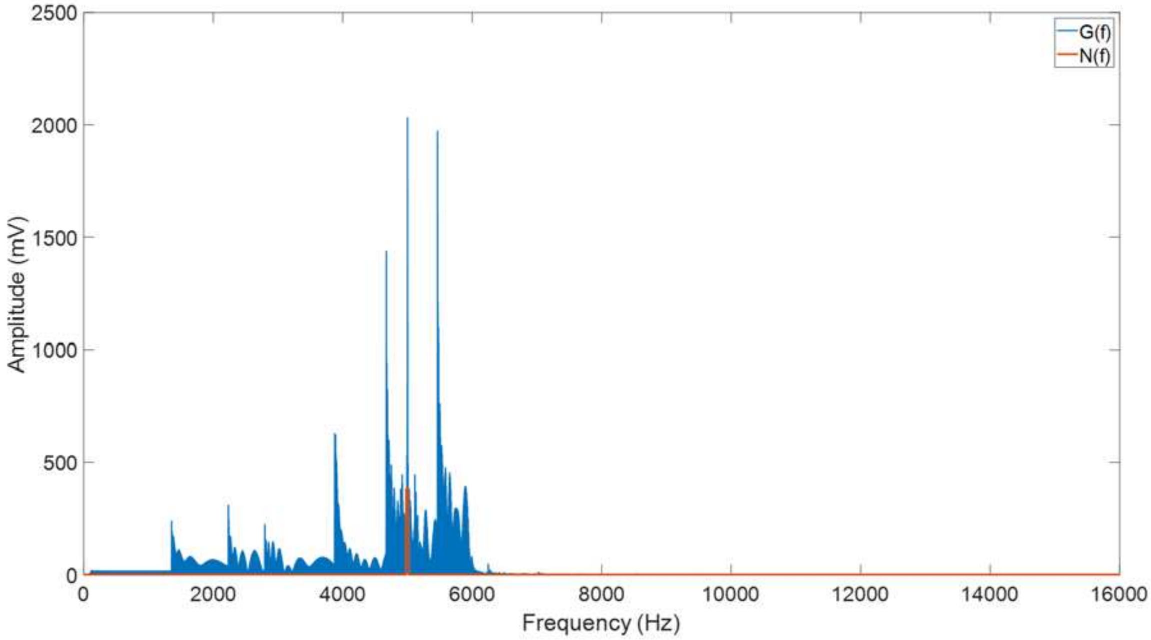

Figure 5. (a) The spectrum of emitted 2ASK signal with 20 Hz bandwidth and 5000 Hz carrier frequency; (b) the spectrum of the communicated 2ASK signal predicted in the pipe 4 m away from the source with additive noise.

Then the deconvolution algorithm was applied to the sequence $\hat{G}(f) + N(f)$ to linearly equalise the undesired effects in the channel and its results can be written as:

$$Y(f) = \frac{X(f)H(f) + N(f)}{H(f) + \mu} \quad (6)$$

where μ is the regulation factor to avoid computational instabilities when the spectral amplitude of $H(f)$ is relatively small. Finally, the output is required to be transformed back to time domain via IFFT, $y(t) = \mathcal{F}^{-1}\{Y(f)\}$, and be ready for the synchronisation.

Deconvolution plays a key role in the in-pipe acoustic communication. The sound wave propagation in a pipe is dispersive when its frequency is higher than 1st cut-off frequency. This phenomenon can cause the signals to stretch and overlap between symbols causing inter-symbol interference (ISI) to occur increasing the difficulty with decoding. At long range communication, the effect of multi-mode propagation will be even more significant. However, the influence of these issues along with additive noise can be linearly equalised by deconvolution. Figure 6 illustrates the 2ASK message pack signal in time domain measured from the experiment before and after deconvolution to show their difference. After deconvolution, the fluctuating of the amplitude of the signal caused by the dispersion has been clearly reduced and quality of the transmitted bits has been significantly improved.

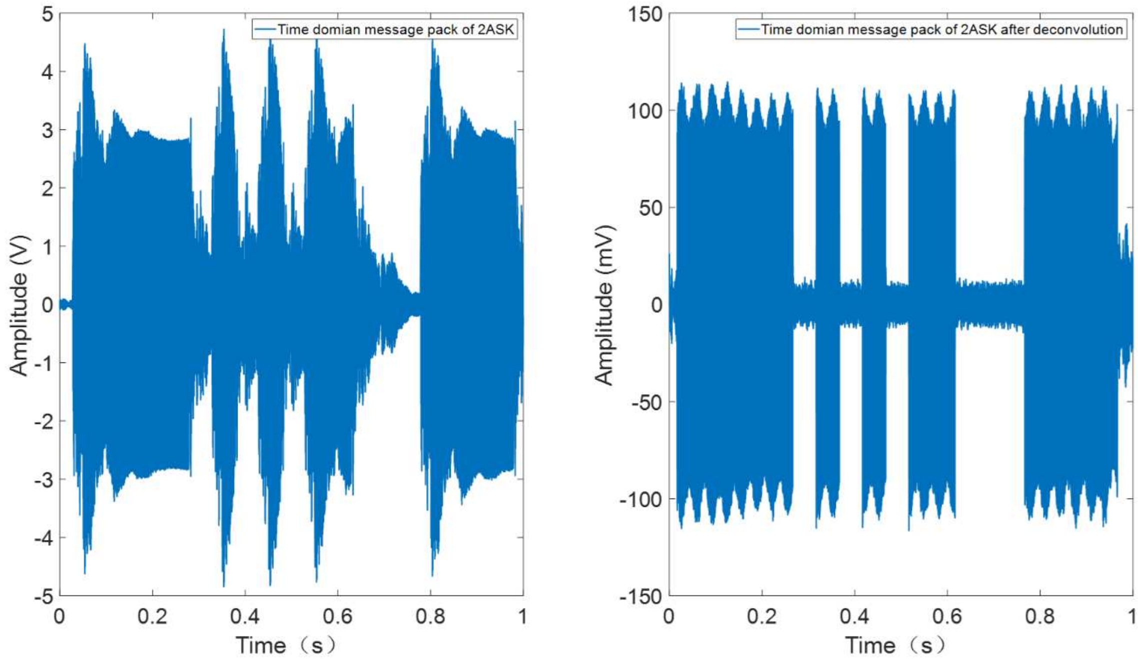

Figure 6. Message pack of 2ASK communication before and after deconvolution

Symbol synchronisation is another key factor that makes the demodulation successful. In this communication system, another useful aspect for the pre- and post-amble is that it can be cross correlated with the same chirp signal stored on board to give two sharp peaks which precisely illustrates the start and end points of the message pack. Figure 7 shows an example of signal synchronisation for the 2ASK communication. In Figure 7 the first and second peak above the threshold red line show the exact starting and ending points of the pre-amble and message pack around 3 seconds and 14.05 seconds, respectively. After cutting off the pre-amble and post-amble, the message pack can be extracted, passed though the filter to remove unwanted frequency components generated by the signal processing algorithm and noise in the channel. According to the adopted modulation technique, the corresponded demodulation method is then applied to decode the message. A parity check is commonly used to make sure that the binary ‘1’s and ‘0’s are not mis-recognised. The final step is to transfer the binaries back to its original form via the so called ‘decoding’ algorithm (see Figure 3).

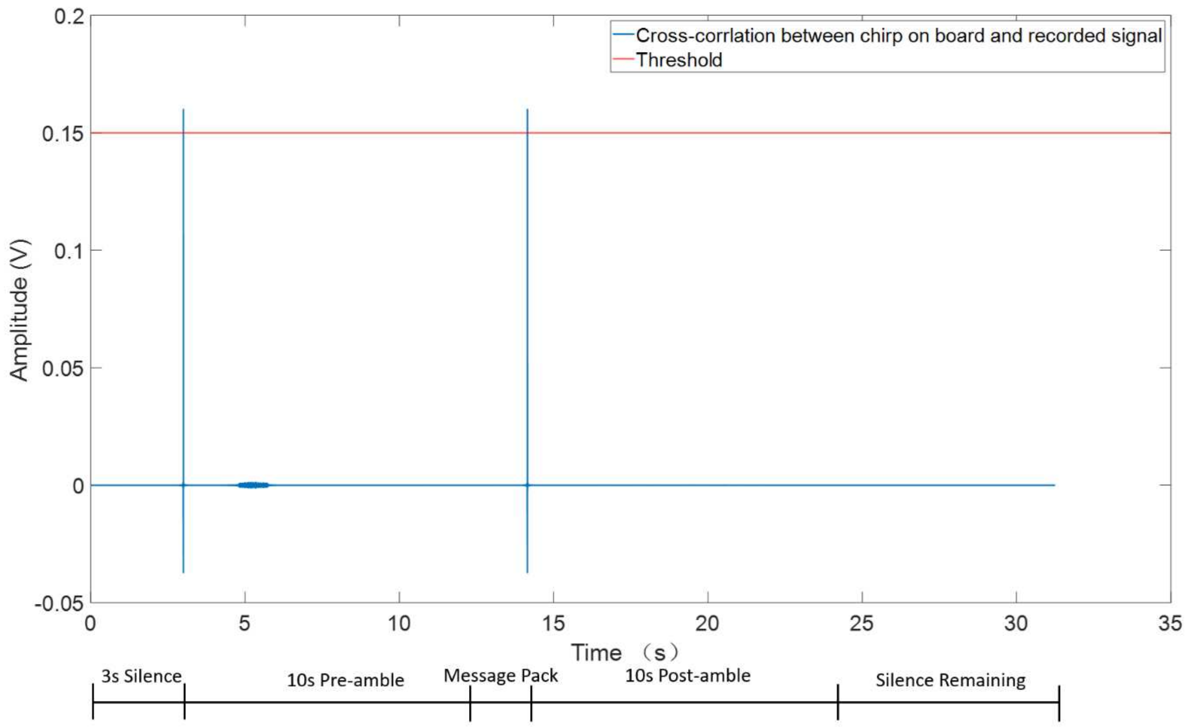

Figure 7. Synchronisation by cross-correlation

4. Modulation & Demodulation (MODEM)

In previous sections, the channel characterisation and common procedures of communications have been introduced. In this section, the four modulation/demodulation technologies will be discussed. This section presents the mathematical expressions and decision making after demodulation.

4.1 Binary Amplitude/Frequency/Phase Shift Keying

These 3 modulation techniques make use of the change in one of the parameters of the sinusoidal carrier wave (i.e., amplitude, frequency or phase) to transmit the digital information, while the rest of two parameters are kept constant. The mathematical expressions of these modulation techniques along with their demodulation techniques have been listed in Table 2.

Name	Signal Modulation	Carrier	Signal Demodulation
2ASK	$e_{2ASK}(t) = \sum_n a_n g(t - nT_B)\, cos\omega_c t$ $a_n = \begin{cases} 1 & probability\ of\ P \\ 0 & probability\ of\ 1-P \end{cases}$	$Acos\omega_c t$	Coherent

	$g(t) = \begin{cases} 1, (n-1)T_B \leq t \leq nT_B \\ 0, t > 0 \mid T > T_B \end{cases}$		
2FSK	$e_{2FSK}(t) = s_1(t)\cos(\omega_1 t + \phi_n) + s_2(t)\cos(\omega_2 t + \theta_n)$ $\begin{matrix} s_1(t) \\ s_2(t) \end{matrix} = \sum_n a_n g(t - nT_B) \cos \begin{matrix} \omega_{c_1} \\ \omega_{c_2} \end{matrix} t$ $a_n = \begin{cases} 1 & probability\ of\ P \\ 0 & probability\ of\ 1-P \end{cases}$ $g(t) = \begin{cases} 1, (n-1)T_B \leq t \leq nT_B \\ 0, t > 0 \mid T > T_B \end{cases}$	$Acos\omega_{c1}t$ & $Acos\omega_{c2}t$	Coherent
2PSK	$e_{2PSK}(t) = \sum_n a_n g(t - nT_B)\ cos\omega_c t$ $a_n = \begin{cases} 1 & probability\ of\ P \\ -1 & probability\ of\ 1-P \end{cases}$	$Acos\omega_c t$ & $Acos\omega_c t + \pi$	Hilbert Transform

Table 2. Mathematical expressions for 2ASK, 2PSK and 2FSK Modem

A typical signal sent through any of the three techniques presented in Table 1 consists of three parts: (i) a_n that is a binary variable switching between two values depending on the position n in the coded sequence; (ii) $g(t - nT_B)$ is the step function which provides the symbol location in coded sequence with the symbol period, T_B, controlled by the modulation frequency, f_M (bandwidth), $T_B = 1/f_M$; and (iii) carrier frequency, $\omega_c = 2\pi f_c$. A 2FSK signal can be treated as composition of two sub-2ASK signals therefore it has two carrier frequencies ω_{c_1} and ω_{c_2} . In a 2ASK signal the variable a_n takes either the value of 0 or 1 to modulate by amplitude. In a 2PSK signal this variable takes the value of 1 or -1, i.e. modulates to modulate by phase ($\pm\pi$). All of these three modulation techniques can be achieved by using on-off keying (OOK) processed on circuits:

$$e_{ook}(t) = \begin{cases} Sending\ '1' & Sending\ "1"s\ by\ probability\ of\ P\ (circuits\ switch\ on) \\ Sending\ '0' & Sending\ "0"s\ by\ probability\ of\ 1-P(circuits\ switch\ off) \end{cases} \quad (7)$$

The most commonly used demodulation approach for binary digital communication is coherent demodulation. The process of coherent demodulation used for 2ASK is illustrated in Figure 8.

This algorithm is to multiply the message pack by its local carrier wave, adding the threshold (normally 50% or so of the peak value for avoiding the threshold effect).

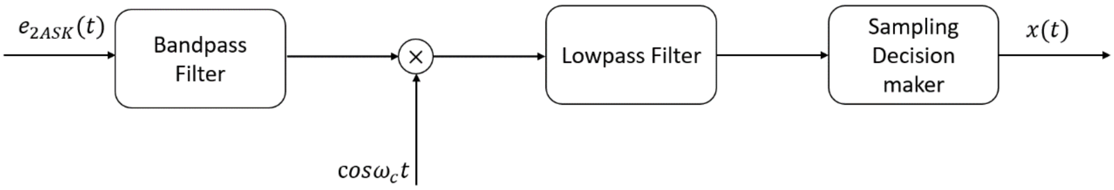

Figure 8. A diagram explaining the process of 2ASK coherent demodulation

However, the coherent demodulation for 2FSK has a difference with that of 2ASK, which has been illustrated in Figure 9. Because a 2FSK signal is consisted by 2 sub-2ASK signal, therefore after synchronisation, the signal $e_{2FSK}(t)$ will be divided in two sub-signals by passing through a bandpass filter. Then their envelops will be picked up by the envelope detectors and in this simulation this step was doing Hilbert Transform. The clocking pulse will help sampling decision maker to judge whether the symbol is '1' or '0'. Finally, the results will be record as the output signal. Another advantage is that either of sub-signal can be checked by another one.

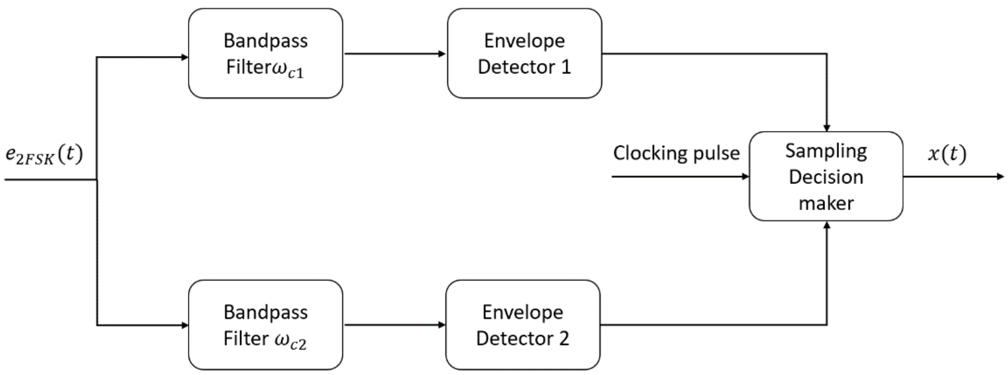

Figure 9. A diagram explaining the process of 2FSK coherent demodulation

In most general cases, coherent demodulation is used for demodulating 2PSK signal. However, in this paper, 2PSK signal will be demodulated in a different way, using angle demodulation:

Recall the general expression of 2PSK signal:

$$e_{2PSK}(t) = Acos(\omega_c t + \varphi_n) \quad (8)$$

and carrier wave with initial phase of zero:

$$e_{carrier}(t) = cos\omega_c t \quad (9)$$

The application of the Hilbert Transform to both (8) and (9) yields two analytic signals:

$$\check{e}_{2PSK} = \mathcal{H}\left(e_{2PSK}(t)\right) = Ae^{i\omega_c t + i\varphi_n} \quad (10)$$

and

$$\check{e}_{carrier} = \mathcal{H}\left(e_{carrier}(t)\right) = e^{i\omega_c t} \quad (11)$$

Then the phase difference between the symbols can be denoted as:

$$\varphi_n = \arg\left\{\frac{H\left(e_{2PSK}(t)\right)}{H(e_{carrier}(t))}\right\} \quad (12)$$

The reason of utilising the angle difference to demodulate the signal is because coherent demodulation highly relies on the adding threshold to the waveform of the demodulated signal. However, any message sent though the acoustic channel in the pipe will suffer the influence of multi-mode propagation and background noise. These effects may cause the waveform distortion which enormously increases the difficulty on decision making in the decoding process, especially under some extreme conditions such as low SNR and long-range transmission. These effects will be specifically discussed in next section. The phase of the signal is relatively stable in comparison to amplitude. Therefore, this feature can be used to differ between '1' and '0' symbols.

Figure 10 shows the decision-making procedure based on adding a threshold to the coherent demodulated signal. This example was selected as a 2ASK signal with the carrier frequency of $5000\ Hz$ and bandwidth of $20\ Hz$ .The blue line is the waveform after demodulation, black circles indicate the sampling points used for decision making and the red line right in the middle (near 50% of the peak value) is the threshold. According to the location of the sampling points, the '1's and '0's can be easily distinguished, and the result of demodulation has identical agreement with the binary sequences contained in excited signal.

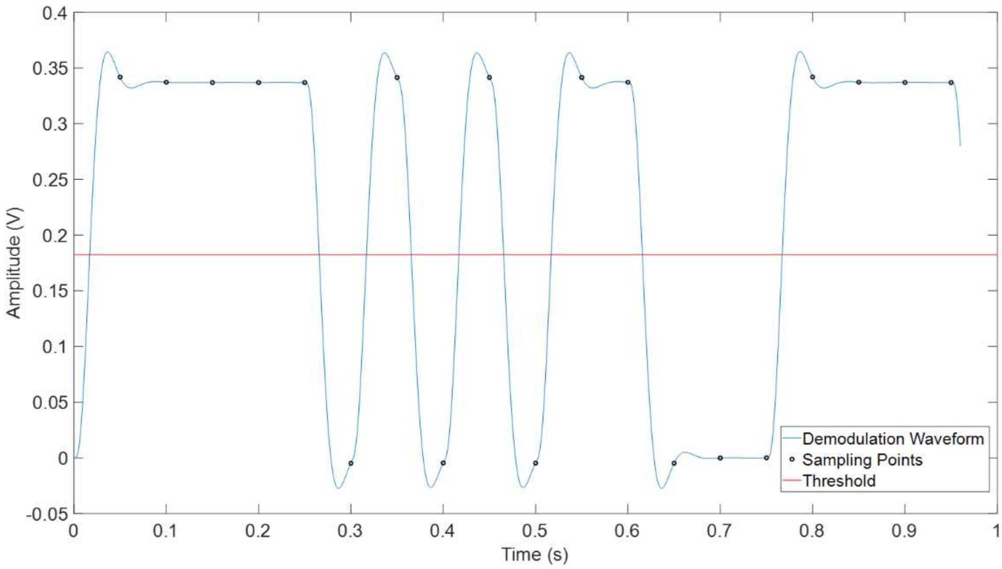

Figure 10. 2ASK coherent demodulation waveform and decision making.

In order to show the difference in decision making process between coherent demodulation and angle demodulation for 2PSK, a special case of decision-making waveform with 3119 Hz carrier, 20 Hz bandwidth under 0 dB SNR has been illustrated in Figure 11 (a).

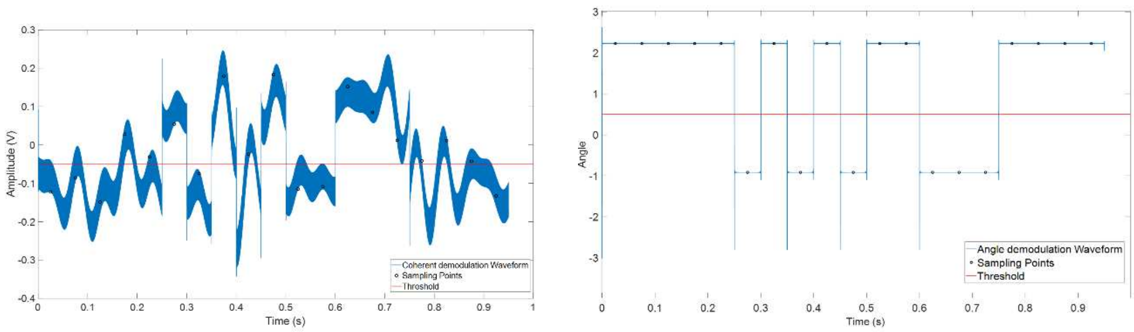

Figure 11. (a) Coherent Demodulation waveform for 2PSK signal (left diagram). (b) Angle demodulation waveform for 2PSK signal (right diagram).

It is very clear in Figure 11 (a) that the waveform was distorted after coherent demodulation and threshold (red line) cannot not be used to make accurate decisions for decoding as a considerable error rate would result. In contrast, angle demodulation gives a clear form of angles as shown in Figure 11(b) and threshold line can be used to accurately decode the signal.

4.2 CLFM

Chirp Linear Frequency Modulation utilises the frequency of the sinusoid chirp from high to low and low to high to form a linearly modulated signal carrying a message. This technique has been widely applied in underwater acoustic communication. [9] have done a considerable amount of work on this technique and demonstrated that it had a great noise resistance to operate in a low SNR environment. Because each symbol in the message is modulated by a sinusoid sweep containing relatively high energy, it is believed that there is also a potential to cope with the effect of multi-mode propagation to become one of the most reliable solution for in-pipe acoustic communication.

4.2.1 Modulation

Similar to the binary Shift Keying technique, CLFM also can be generated by OOK technique (on-off keying). However, in order to prevent the mis-synchronisation and ISI (Inter-symbol Interference) during the demodulation short (e.g. 0.001 s) short intervals are added between each symbol.

$$e_{CLFM} = s(t)\ A\ sin(2\pi f(t)t + \phi_0) \tag{13}$$

where $s(t)$ is given by Table II. The transient frequency in eq. (13) can be expressed as: $f_{\pm}(t) = f_0 \pm kt$ and $k = \frac{f_1 - f_0}{T}$, f_1 and f_0 are the start and end frequency for the chirp and T is the period of e_{CLFM}. Therefore, the general form of CLFM can be written as:

$$e_{CLFM}(t) = \begin{cases} Asin(2\pi f_+(t)t + \phi_0) & Sending\ "1"s \\ Asin(2\pi f_-(t)t + \phi_0) & Sending\ "0"s \end{cases} \tag{14}$$

In addition, the initial phase for the CLFM ϕ_0 can be set to 0. Figure 12 illustrates an example of the message pack for CLFM generated by OOK. In this example, the frequency range was chosen from 1500 Hz to 5000 Hz. Two graphs in the middle are single chirp components which represent ‘1’s and ‘0’s and a 0.01s interval behind and last graph is the final waveform after the modulation.

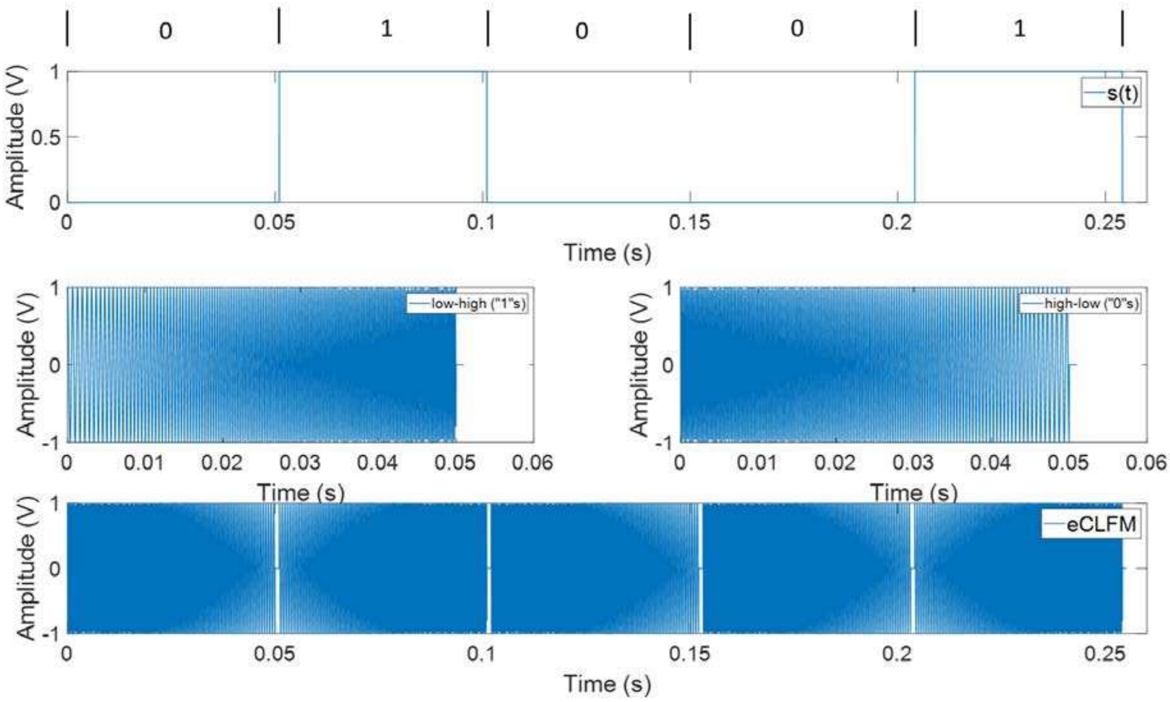

Figure 12. An illustration of key stages in the CLFM modulation process: (Top diagram) Square wave $s(t)$ to show the binary change of sending "1" s and "0"s. (Two middle diagrams) Sub-chips with frequency from low to high and high to low. (Bottom diagram) modulated CLFM signal.

4.2.2 Demodulation and Decoding

Different to the traditional demodulation process, CLFM utilises the cross-correlation approach to distinguish between '1's and '0's in the message pack. The technique is to store the two chirp signals on board and then cross-correlate them with the whole message pack signal on the receiving end. By doing so, the symbol which has high relevance will illustrate a high correlation with the right chirp whereas the cross-correlation results of the other chirp will be very low. Figure 13 (a) illustrates CLFM demodulation results under the SNR of 50 dB, symbol period is 0.05 s and frequency range for the sub-chirps is between 4000 Hz and 5000 Hz.

Figure 13 (b) and (c) show that the decision making can be based on detecting whether or not the sharp correlation maximum is within the time window. In addition, the peak value in Figure 13 (c) is around 0.8 mV which is nearly 4 times as much as the averaging value in Figure 13 (c), therefore this modulation technique has very good noise resistance. The noise resistance can be further improved by widening the frequency range of the sub-chirps and symbol period even though it will cost the data transmission speed.

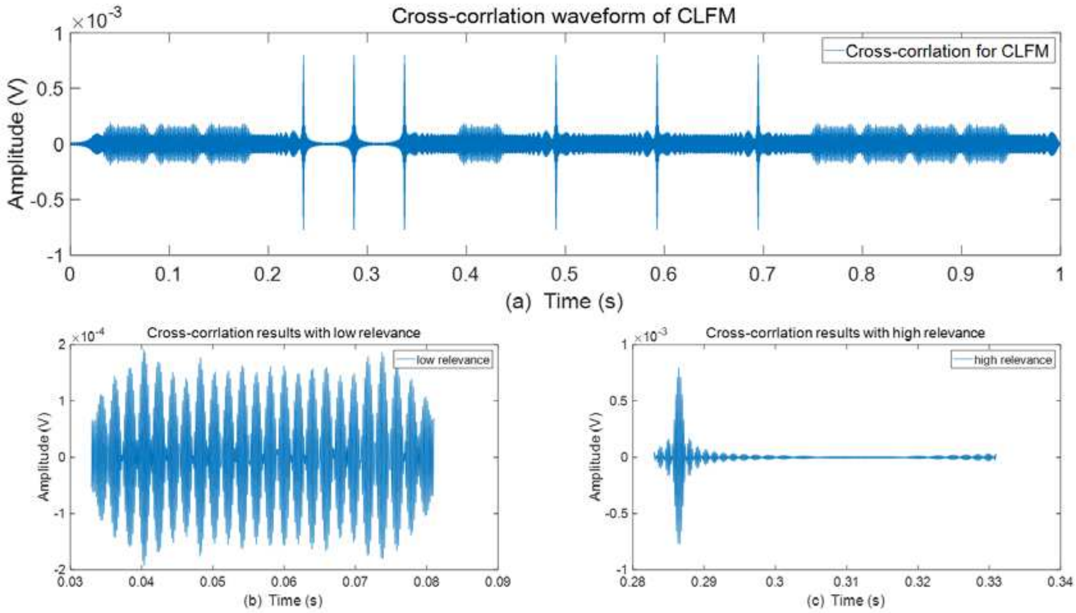

Figure 13. (a) Cross-correlation results for CLFM. (b) Signal in window with high relevance. (c) Signal in the window with low relevance.

5 Simulation and Experimental Validation

The last two sections discuss the importance of channel characterisation to support the four communication techniques to work in pipes. It was noted there may be some issues while transmitting information in the pipe at a carrier frequency that is higher than first cut-off frequency of the pipe. At these frequencies the sound wave is no longer be a plane wave as it propagates in a plurality of way (multi-mode propagation) causing the signal to spread. Such phenomenon is likely to lead to some inter-symbol interference and increase in the number of error bits. Another reason for error bits is the wide band additive noise. It is generally believed that in real partially filled pipes, e.g. sewers and drainage pipes, there is a considerable amount of noise generated by the road traffic, water flow and nearby industrial installations. The effect of this noise on the quality of communication cannot be ignored. Finally, it also should be noticed that the communication range and communication speed are directly rely on the sound attenuation in the pipe. This section will focus on these challenges and explore how the 4 systems cope with them by simulation and experimental studies.

5.1 The effect of SNR

5.1.1 Through the Simulation

The reliability of each of the four communication techniques under different SNRs was tested through simulation by using the analytical model and measured response of the pipe. This evaluation was based on comparing the probability of package error rate (PER) for the four techniques as a function of the SNR and carrier frequency predicted through the signal processing algorithm described in section 2.

Firstly, the carrier frequency and modulation frequency were keeping constant, but SNR was varied between -30 dB and 20 dB. The PER was calculated as:

$$PER = \frac{N_{error}}{N_{total}} \tag{15}$$

where N_{error} is the number of error bits and N_{total} is the total number of bits in the message pack. In this simulation the length of the message pack was set to 19 bit which contained 15 random binary information bits and 4 extra parity check bits. For each type of system, the test was repeated 200 times. Each time the information bits were randomly changed, message was decoded, decoded messaged was compared to that initially sent and PER was calculated according to Eq. (15). The PER for each of the 200 runs were averaged to ensure that the final result makes good statistical sense.

In this study, the modulation frequency was chosen as 20 Hz, carrier frequency of 5000 Hz for 2AKS, 2FSK and 2PSK. The frequency of the modulation chirp for the CLFM was set in range between 4000 Hz and 5000 Hz. The reason for choosing this setup was that 20 Hz narrow band modulation could give relatively good noise resistance which ensured that the system was tested under a relatively low SNRs. This relatively low bit rate is sufficient for autonomous robots to communicate messages related to their location inside the pipe and operational status. The choice of the frequency range around 5000 Hz was based on the balance between the sound attenuation which increases with the frequency and number of carrier frequency period required to modulate a message with the bits transmitted at 20 Hz. The relation among attenuation, communication range and communication speed will be specifically discussed in the next section.

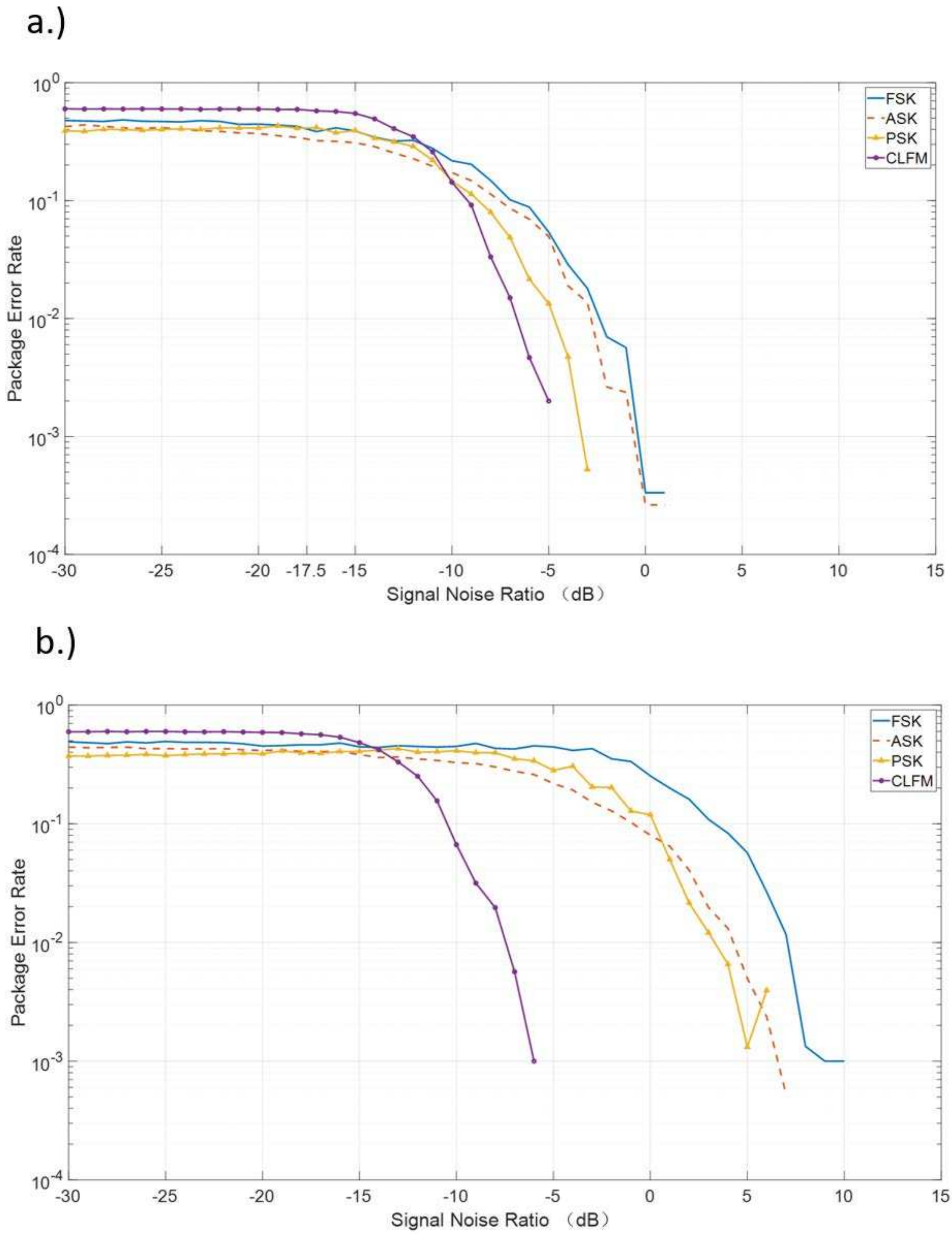

Figure 14. A diagram illustrating the PER for the four communicaiton technologies with 20Hz modulation frequency (5000 Hz carrier frequency for 2ASK, 2PSK, 2FSK and 4000Hz-5000Hz

modualtion chirp for CLFM) as a function of the SNR for: (a) FRF predicted theoretically; (b) measured FRF.

Figure 14 presents the package error rate as a function of the SNR. These are simulated results obtained for the four communication techniques making use of the predicted frequency response function (FRF) (Figure 14 (a)) and experimentally measured FRF (Figure 14 (b)) for a dry 150 mm diameter pipe. The model and experiments were detailed in sections 2. These FRFs were used in the deconvolution to improve the quality of the signal with coded message (see section 3).

The results presented in Figure 14 suggest that the package error rate (PER) depends strongly on the SNR. There is some difference in the PER behaviour simulated with the two FRFs. According to these results, the quality of the communication channel simulated with the predicted FRF (Figure 14 (top)) improves more rapidly with the increased SNR than in the case when the FRF was measured (Figure 14 (b)). Also, the difference in the performance of the four communication techniques seems relatively small in the case when the FRF was predicted (around 5 dB between CLFM and 2FSK to reach 1% probability). The pattern in the behaviour of the PER as a function of the SNR is similar for all the four communication techniques. When the SNR reaches certain level, the PER begins to drop exponentially. For relatively low SNRs the PER reaches its theoretical limit of around 50%. In the case when the FRF was measured, the best performing technique by far was the CLFM (see Figure 14 (b)). This technique enables to reach a PER = 1% at SNR = -7.5 dB. This is almost 15 dB better than that simulated for the 2FSK. The performance of the 2ASK and 2PSK was found similar and between that calculated for the CLFM and 2FSK.

There are other conclusions. Firstly, increasing the SNR can improve the quality of cross-correlation which is helpful to reduce the PER for the CLFM further. Secondly, the PER of the 2FSK, 2ASK and 2PSK techniques drops relatively fast with the increased SNR suggesting that these three modulation techniques can be more easily affected by the complexity of the pipe and ambient noise present. In real applications, these three techniques would require a relatively high SNR to transmit data accurately, i.e. at a very low error rate. In the case of the CLFM there a relatively little difference was found between the PER obtained with the theoretically predicted FRF and measured FRF (see Figure 14).

5.1.2 Through the experiment

In this section, the overall performances of four communication techniques simulated with the theoretical model (section 2, sub-section 2.1) are compared against the communication data obtained experimentally. The signals used in the experiment with the four communication techniques were identical to those used in the simulations. The full characteristics of these signals are described in sections 3 and 4. Examples of these signals can be found in our supplementary data via the link provided in the Appendix. The message signal was emitted by the loudspeaker and received on the microphone using the experimental setup shown schematically in Figure 2. The distance between speaker and microphone was set to 10 m. The recorded signal was processed accordingly, demodulated and decoded using the methods explained in Section 4 to study the effect of the background noise on the PER. The initial SNR in the experiment was estimated as 45 dB and this value was used subsequently as the reference representing the 'no noise condition'. The SNR was reduced progressively to -30 dB by introducing of artificial background noise. For each SNR the measurement was repeated 3 times, PER value for each of these measurements was calculated, and their average was presented as a final result.

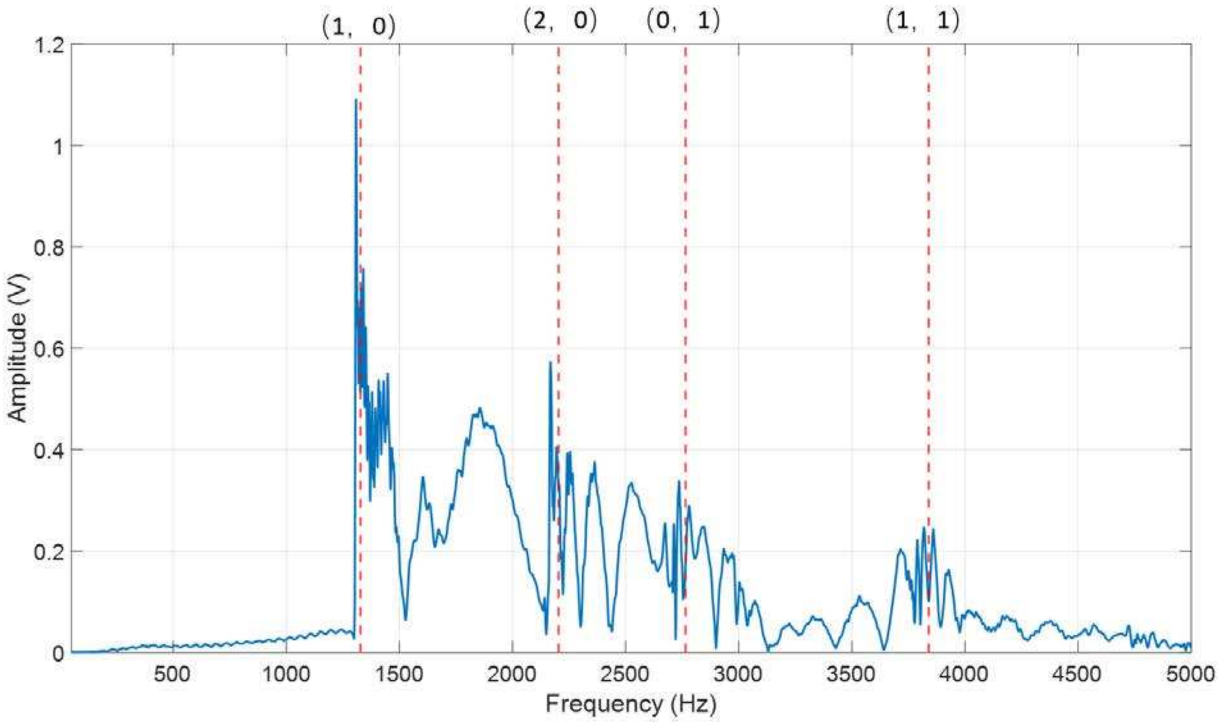

Figure 15. Measured FRF of 150 mm diameter pipe (blue lines) and 4 cut-off frequencies (red dash lines).

Figure 15 plots the experimentally measured FRF for 150 mm diameter pipe in blue line and 4 cut-off frequencies has been marked in red dash lines. These cut-off frequencies $f_{cut-off}$ were calculated by equation:

$$f_{cut-off} = k_{mn} \frac{c_0}{2\pi r} \tag{16}$$

where k_{mn} is modal wavenumber c_0 is sound speed and r is radius of the pipe. It can be suggested that the measured FRF has the clear peak which has the close agreement with the theoretical cut-off frequencies.

The measured PER as a function of the SNR for each of the four communication techniques is shown in Figure 16. This figure confirms that the CLFM is the most robust communication technique in terms of its ability to cope with the background noise. The experimentally obtained PER for this technique reduces slightly slower than that calculated using the measured and simulated FRF. The difference in performance between these cases is close to 5 dB (see Figure 14 (top) and 16). This 5 dB decrease can be caused by the pipe ends, imperfect seals in the connections between the pipe sections. There also can be some differences associated with the microphone and speaker response attained at the time of the two sets of experiments. Even though the deconvolution method cancelled the influence of these factors to some extent, it may not be fully reliable for lower SNRs. Similar discrepancies were observed when the other three communication techniques were validated experimentally.

The results shown in Figures 14 and 16 generally support the predictions obtained through the simulation. The acoustic signal passing through the pipe experiences strong multi-mode propagation. When the pipe has a finite length, the influence of multi-path effect and reflections caused by the open ends and connections is hard to predict and can affect the quality of communication significantly. They deserve more attention through more refined simulations and better controlled experiments. Those undesirable channel properties can be potentially equalised by applying deconvolution with the right FRF. Among the proposed four communication techniques the CLFM was observed to have the best noise resistance with the PER = 1% at SNR = -1.5 dB. This performance was attained with the 2ASK, 2PSK and 2FSK at SNR = 4, 7.5 and 8 dB, respectively.

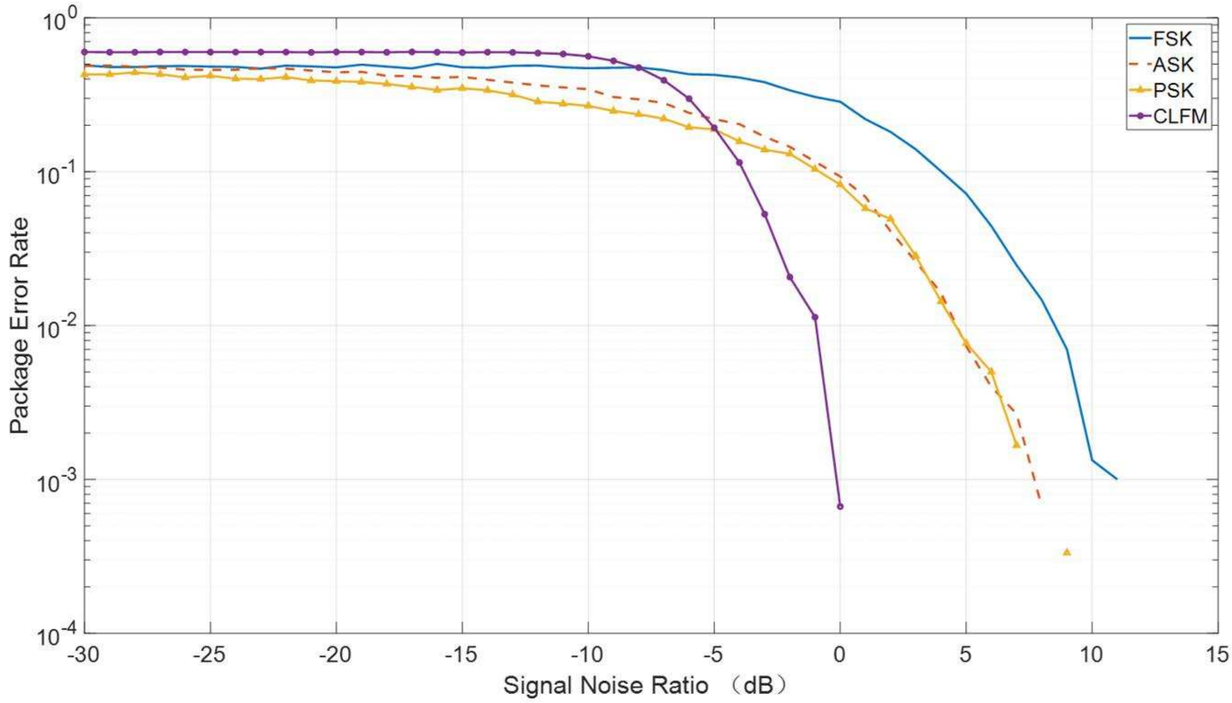

Figure 16. Diagram illustrates the experimental validation for comparison of 4 communication systems with 20Hz modulation frequency and 5000 Hz carrier frequency and 4000Hz~5000Hz modulation chirp for CLFM under SNR in the range between -30dB~20dB

5.2 The effect of carrier frequency

In section 2 it was noted that a pipe supports a number of modes which can be excited when the carrier frequency exceeds a certain threshold called the cut-off frequency. Beyond this frequency sound propagation is multi-modal and dispersive causing the waveform with the message to stretch and distort. A simulation was carried out to determine the relation between the carrier frequency and PER. In order to give a better view of this relation, the carrier frequency was nondimensionalised to the product of wavenumber and radius of the pipe:

$$kr = \frac{2\pi f_c}{c_0} \tag{17}$$

This simulation also was repeated 200 times to make sure the results are statically reliable. The bandwidth f_m was set to 20Hz and SNR was set as 0dB. The testing range of carrier frequency f_c was set from 500 Hz to 5000 Hz for the 2ASK, 2FSK and 2PSK. However, these settings are different for CLFM. We define the frequency range for sub-chirp as: [$f_{central}$-500 Hz, $f_{central}$+500 Hz], where $f_{central}$ is the middle frequency of the sub-chirp frequency range. For example, in the case of a sub-chirp with $f_{central}$ of 1200 Hz the frequency range was set form

700 Hz to 1700 Hz. The sub-chirp frequency range can be controlled by step-changing of $f_{cnetral}$. Similar to the settings for f_c, the testing range of $f_{central}$ was set from 800 Hz to 4500 Hz.

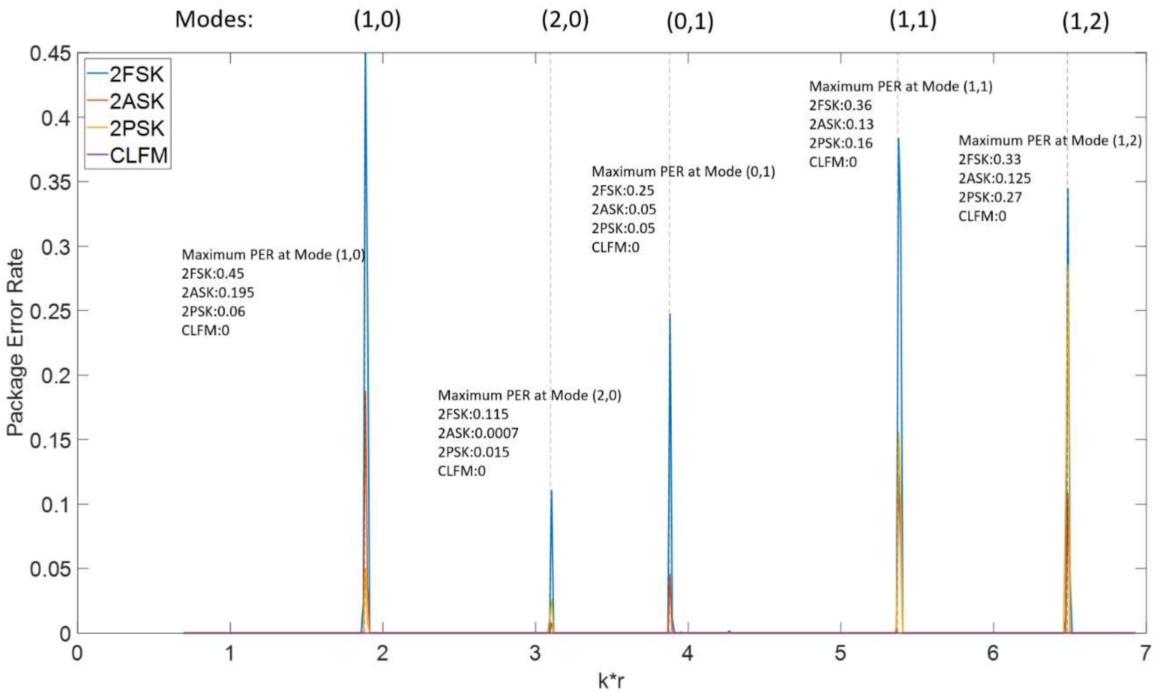

Figure 17. A diagram showing the dependence of the PER on the dimensionless frequency for SNR = 0 dB and f_m = 20 Hz.

Figure 17 illustrates the results of this simulation. The modal frequencies are marked as grey dash lines. As it has been deduced previously, sending message at the carrier frequency close to a modal frequency result in a high possibility to cause a high package error rate close to its theoretical maximum. Therefore, it should be suggested that carrier frequency of in-pipe acoustic communication should be chosen to avoid being close to a cut-off frequency. Similar to the results shown in Figures 17 the 2FSK was found the most unstable among the four communication techniques when the carrier frequency is close to a cut-off frequency. The 2PSK was ranked the second most unstable technique and 2ASK works slightly better than the latter two. Most importantly, the PER of the CLFM remained close to 0 though the entire simulation which not only determine that this technique is able to overcome the effects of modes but also validate that compare with the 2ASK, 2PSK and 2FSK, it has the best noise resistance.

5.3 Communication Speed Evaluation

In digital communication, the speed of information transmission is calculated by bit rate (bps): $R_b = \frac{n}{T_m}$. The index n denotes the number of bits contained in the message pack and T_m is the period/duration of the message pack. In binary modulation one symbol period $\frac{1}{f_M}$ only represents one bit and bit rate R_b is also equal to the modulation frequency f_M. Increasing the bit rate can be achieved through a higher modulation frequency. However, doing so would require wider bandwidth in frequency domain. Therefore, the carrier frequency f_c needs to be as high as possible to ensure there will be sufficient blank space for the wide band communication.

For 2ASK and 2PSK, the bandwidths are as twice as the symbol rate, therefore they have:

$$B_{2ASK/2PSK} = 2f_M \tag{18}$$

so that the maximum bit rate for 2ASK and 2PSK system is:

$$R_{b_{2ASK/2PSK}}|_{max} = \frac{1}{2}f_c \tag{19}$$

In the case of the 2FSK 2 sub-carriers are adopted so that its bandwidth can be approximated with:

$$B_{2FSK} = |f_2 - f_1| + 2f_M \tag{20}$$

and

$$f_2 - f_1 > f_M \tag{21}$$

The centre frequency of this band is:

$$f_{centre} = \frac{f_1 + f_2}{2} \tag{22}$$

Let us assume that f_1 is always lower than f_2. Then we have:

$$\frac{f_1 + f_2}{2} > f_2 - f_1 + 2f_m \tag{23}$$

$$R_{b_{2FSK}} = f_M < \frac{f_1}{2} \tag{24}$$

Thus, combine eq. (21) and Eq. (24), the maximum bit rate for the 2FSK is half of lower sub-carrier frequency while $f_2 = \frac{3}{2}f_1$.

In the case of CLFM the carrier wave is a chirp signal which spectrum covers a range of frequencies. In principle, its bandwidth could be infinitely wide and therefore the CLFM is also a spreading spectrum communication technique. However, according to the Nyquist sampling law:$f_{c_{max}} < \frac{1}{2} f_{sampling}$, the maximum frequency in the chirp should lower than the half of the sampling frequency. In addition, there are a time interval T_{int} between each symbol to avoid neighbour symbol overlap. In this case the total message pack period $T_{message}$ will need to be:

$$T_{message} = \lim_{N \to \infty} (\frac{1}{R_b} N + T_{int}(N-1)) \quad (25)$$

where N is the number of symbols in the message package. For the purpose of cancelling the ISI caused by the multi-mode propagation T_{int} should be based on:

$$T_{int} = \frac{z}{c_g} \quad (26)$$

In equation (26), z is the distance between the source and receiver and c_g is group velocity of the waveguide and the actual bit rate for CLFM is：

$$R_b|_{actual} = \frac{T_{message}}{N} \quad (27)$$

The group velocity is usually frequency depended in a multi-modal pipe. It is very clear that attempting to fully avoid ISI will sacrifice the communication speed and for the short range and period communication, the influence of time interval can be ignored while in long range and period message transmission, this effect has to be taken into account.

The attenuation of sound in a pipe is not a negligible issue particularly for high frequency carrier wave typical for acoustic communication. If the pipe wall is rigid, then the sound pressure in cylinder reduces due to the frequency-dependent air absorption:

$$p(\omega) = \sum A_m J_m(k_{mn} r)\, e^{j(\omega t - k_z z + j\alpha)} \quad (28)$$

where the α is the attenuation coefficient which can be obtained from:

$$\alpha = \frac{\omega^2}{2\rho_0 c^3} [\frac{4}{3}\eta' + \chi\left(\frac{1}{C_V} - \frac{1}{C_P}\right) + \sum_{i=1}^{n} \frac{\eta_i''}{1+\omega^2\tau_i^2}] \quad (29)$$

In eq. (29), η' and η_i'' are the shear and volumetric viscosity of the air, respectively. C_V and C_P are the specific heat capacity at constant volume and pressure, χ is the heat conductivity and τ_i is shear force in the vibrational relaxation process. According to eqs. (32) and (33), the sound attenuation is mainly affected by two parameters: attenuation coefficient and distance between the source and microphone while the former is a frequency dependent quantity.

In addition to the attenuation caused by air absorption, there is attenuation caused by the visco-thermal effects in the fluid that is not negligible because of the finite values of the fluid viscosity and thermal conductivity. A model has been developed to account for the visco-thermal losses at the duct walls (e.g. Lahiri et al [12]). The attenuation coefficient for these losses is:

$$\alpha_{wall} = \frac{1}{Rc}\sqrt{\frac{\upsilon\omega}{2}} + \frac{\gamma - 1}{Rc}\sqrt{\frac{\chi\omega}{2}} \quad (30)$$

where R is radius of the pipe, υ is kinematic viscosity, γ is heat capacity ratio and χ is thermal diffusivity $\chi = \kappa/\rho C_P$ and κ is heat conductivity of air. The terms $\frac{1}{Rc}\sqrt{\frac{\upsilon\omega}{2}}$ and $\frac{\gamma-1}{Rc}\sqrt{\frac{\chi\omega}{2}}$ are the separate attenuation coefficients caused by viscosity and thermal conductivity losses at wall, respectively. Equation (30) is based on the assumptions of plane wave and wide tube. It can be found from equation (30) that α_{wall} is both frequency-dependent and diameter dependent and increases with the value of $\sqrt{\omega}$.

Figure 18 illustrates the frequency-dependent attenuation caused by the air absorption and visco-thermal effects in the frequency range of 0 Hz to 15000 Hz. The properties used to estimate α_{air} and α_{wall} were chosen that of air under STP and the radius of pipe was $0.075\ m$. In this calculation, the relative humidity was set to 50%.

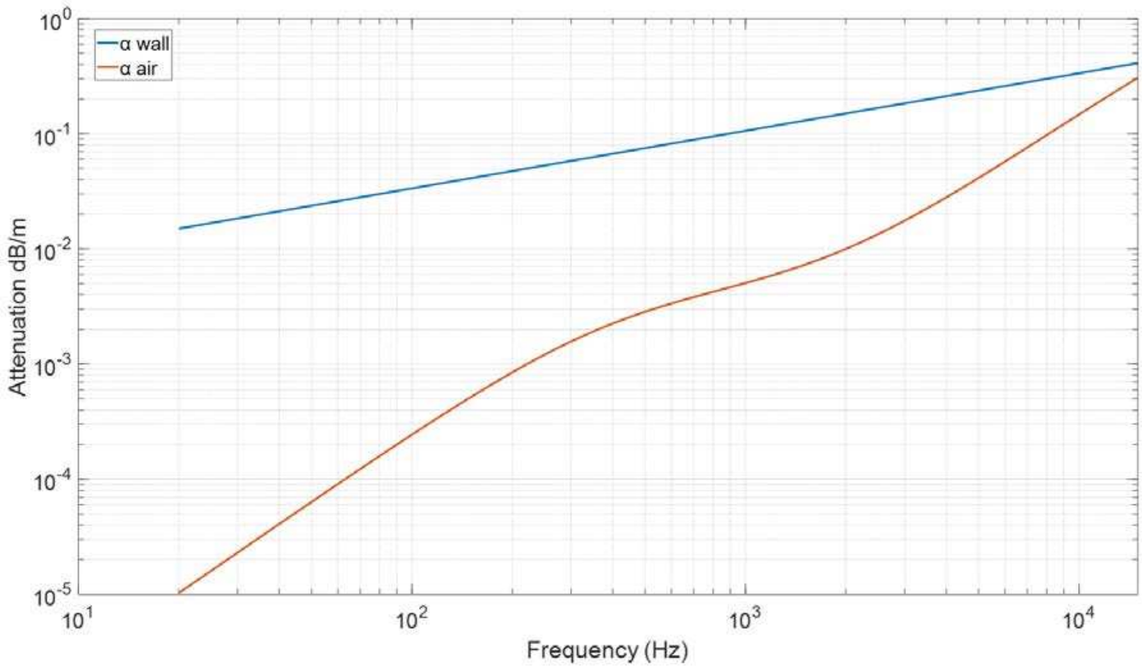

Figure 18 A comparison between the attenuation coefficients caused by the visco-thermal effects at the wall and air absorption in the pipe. The results shown in Figure 18 suggest that α_{air} and α_{wall} rise

with the increased frequency. The attenuation caused by the visco-thermal effects is up to a hundred times higher than that caused by the air absorption in the frequency range between $10\ Hz \sim 1000\ Hz$. However, they are getting closer in higher frequency range which denotes that in lower frequency range, the attenuation is dominated by the value α_{wall} and with the increase of the frequency, the impact of α_{air} is getting stronger and much obvious.

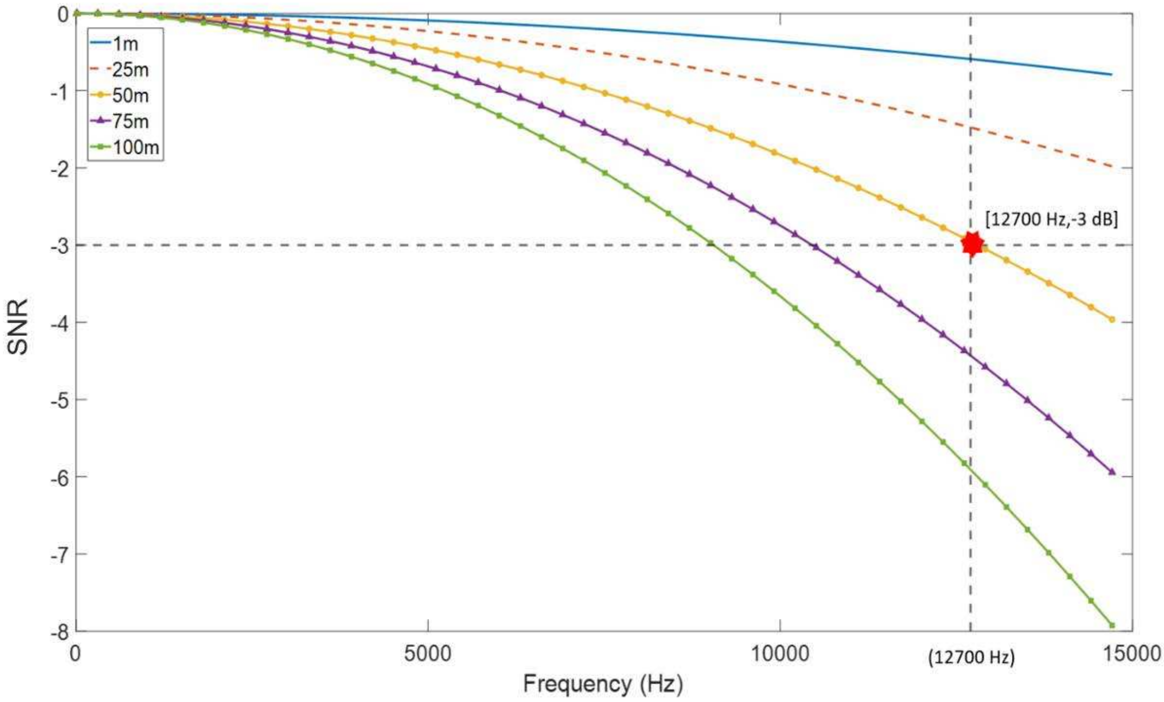

Figure 19. The diagram illustrating the sound attenuation as a function of frequency.

Pipe wall roughness is another source of attenuation. There is a limited experimental data on the effect of wall roughness. The work by Horoshenkov et al [13] estimates that the attenuation in a 600 mm diameter concrete pipe increases with the wall roughness and it is frequency-dependent. If the pipe is empty, it is comparable with that expected from the visco-thermal effects (see Figure 18). An addition of rigid scatterers increases the pipe roughness and this effect is particularly noticeable in the frequency range below 300 Hz (see Figure 4-6 in ref. [13]). A considerable increase in the attenuation can be observed if the wall of the pipe is covered with a porous layer as demonstrated in ref. [14]. In this case the attenuation at higher frequencies of sound (well above the first cut-off frequency of the pipe) can more than treble (see Figure 5 in ref. [14]). This effect is complex, parochial to the wall boundary conditions and usually predicted with a finite element model [14]. Therefore, it is studied in this paper.

Figure 19 gives a graphical estimation of the frequency-dependent signal-to-noise ratio due to the air absorption and visco-thermal effects on the pipe wall. The pipe roughness effects are not considered here. Five lines with different colour denote different distances (1-100m) between the sound source and microphone. The range of the carrier frequency was set below 15 kHz. According to figure 19, when the source and receiver are 1-25 m apart, the effect of attenuation is relatively small. If the communication range is extended to 25 m, then the sound pressure of 1500 Hz carrier wave would drop by only 2 dB. If the speaker is 100 m away from the microphone, then the sound pressure would drop by 6-8 dB at frequencies above 12 kHz. This drop is more noticeable. It has been suggested in previous sections that a low SNR would lead the increase of bit error rate. The intersection with the horizontal grey dash line in figure 19 shows the frequency and range at which the attenuation becomes greater than 3 dB. For example, at the 50m range this happens when the carrier frequency reaches 12700 Hz. Furthermore, the theoretical maximum communication speed for 4 systems can be estimated accordingly by the equation (22), (27) and (30) and has been listed in Table 3:

Communication Techniques	Carrier Frequency f_c (Hz)	Modulation Frequency f_m (Hz)	Bit Rate R_b (bps)
2FSK	f_1=8466, f_2=12700	4233	4233
2ASK	12700	6350	6350
2PSK	12700	6350	6350
CLFM	0~12700	6350	6.82

Table 3. Comparison among 4 communication systems when they are approaching their highest data transmission speed.

Among the proposed four communication technologies 2ASK and 2PSK in 50 m distance have highest data transmission speed of 6350 bits/s. 2FSK ranked the third position with 4233 bits/s and due to the limitation of inter-symbol intervals, CLFM has lowest speed of only 6.82 bits/s. These figures will reduce if the wall of the pipe is no longer smooth and rigid because of extra attenuation [13,14]. This will have an impact on the package error rate and communication range.

6. Conclusions

This paper has studied the importance of the acoustic channel characterisation for communication in an air-filled pipe. This has been illustrated by using analytical and experimental approaches. The pipe used in this work as an example is a typical pipe used to remove wastewater from domestic premises. The performance of four communication techniques, 2ASK,2PSK, 2FSK and CLFM, has been studied. These techniques can be potentially deployed on robots inspecting the pipe collaboratively and autonomously. The capabilities of these four techniques against noise and uncertainties such as multi-mode propagation in the pipe have been tested through simulation and experiment.

The predicted performance of 2ASK, 2PSK and 2FSK modulation is good when the SNR is higher than 0 dB while the experimental validation suggests that the ideal SNR for these three techniques should be in the range between 7 dB and 15 dB. Therefore, it can be deduced that 2ASK, 2PSK and 2FSK are easily affected by the noise and uncertainties in the pipe properties and geometry assumed in the model. These communication techniques need a relatively high SNR to function properly in real application. It has been found through simulation and experiment that CLFM is the most stable technique among the 4 to operate at low SNRs, e.g. -5 - 0 dB.

The influence of the modes on the quality of communication can be significant. Sending message at frequencies close to modal is likely increase the bit error rate. The use of the channel FRF in deconvolution can reduce the effect of the modes. It makes sense to demand that the career frequency should not be selected close to a modal frequency when using 2ASK, 2PSK and 2FSK communication techniques. This seems less of an issue when using the CLFM technique.

The sound attenuation in the pipe due to the air absorption and visco-thermal effect can cause the reduction in the SNR and negatively affect the bit error rate. One can expect a 3 dB attenuation at 50 m when communicating at the 12700 Hz carrier frequency. Based on this information it is possible to estimate the highest communication speed. It has been found that 2ASK and 2PSK techniques would work up to 50 m distance with the maximum transmission speed of 6350 bps. 2FSK has been ranked at the third position with 4233 bps and even though CLFM is the most reliable system, due to the effect of inter-symbol intervals, it has had the lowest communication speed which is only 6.82 bps.

There is still some scope for more work. This paper only studied dry, round pipe. In a real drainage or sewer system there would be uncertainties such as flow, junctions, manholes, sedimentation and other artefacts. Pipe wall can be inherently rough or covered with absorbing layer that can affect the acoustic attenuation of the pipe. These conditions need to be investigated properly because they are likely to affect the FRF and communication speed. In particular, it has been shown [8] that changing the water level shifts the modal frequencies in which case the carrier frequency may need changing accordingly to avoid problems discussed in section 3. This paper used four particular communication techniques for which noise resistance and bit rates can be limited. In the future, advanced technologies such as 4G can be applied to improve these performances. Finally, in practical application, duplexing and CDMA are two key functions which can be achieved in further studies.

Acknowledgement

This work is supported by the UK's Engineering and Physical Sciences Research Council (EPSRC) Programme Grant EP/S016813/1 [1]. The authors are very grateful to Mr. Paul Osborne and Dr. Andrew Nichols for the help with software and experimental setup. In addition, the special thanks to Dr. Viktor Doychinov (University of Bradford) for his help on methodology. For the purpose of open access, the author has applied a 'Creative Commons Attribution (CC BY) licence to any Author Accepted Manuscript version arising'.

Author Contribution

Zhengwei Li: Experimental Work, Formal Analysis and Original Draft Preparation. **Yicheng Yu**: Experimental Work, Data Analysis and Reviewing. **Kirill Horoshenkov**: Supervision, Writing and Reviewing

References

[1] Pipebots, “Pervasive Sensing of Buried Pipes,” 2019. [Online]. Available: https://pipebots.ac.uk/.

[2] C. Parrott, T. Dodd, J. Boxall and K. Horoshenkov, “Simulation of the behavior of biologically-inspired swarm robots for the autonomous inspection of buried pipes,” *Tunnelling and Underground Space Technology,* 27 April 2020.

[3] I. F.Akyildiz and E. P.Stuntebeck, “Wireless underground sensor networks: Research challenges,” *Ad Hoc Networks,* pp. 669-686, November 2006.

[4] Y. Li, “Experimental study on ultrasonic signal transmission within the water-filled pipes,” in *Mechatronics and Machine Vision in Practice, Proceedings, Fourth Annual Conference*, 1997.

[5] G. Kokossalakis, “Acoustic Data Communication System for In-Pipe Wireless Sensor Networks,” Ph.D. dissertation, Massachusetts Institute of Technology, Cambridge,MA,USA, 2006.

[6] L. Jing, Z. Li, Y. Li and R. D. Murch, “Channel characterization of acoustic waveguides consisting of straight gas and water pipelines,” *IEEE Access ,* vol. 6 , pp. 6807-6819, 2018.

[7] L. Jing, M. Wang and Y. Lu, “Differential orthogonal frequency division multiplexing communication in water pipeline channels,” *The Journal of the Acoustical Society of America,* pp. 129-134, 04 August 2020.

[8] Y. Yu, A. Krynkin, L. Zhengwei and K. Horoshenkov, “Analytical and empirical models for the acoustic dispersion relations in partially filled water pipes,” *Applied Acoustics,* pp. 179-193, 26 March 2021.

[9] C. C. Tsimenidis, B. Sherlock and J. A. Neasham, “Spread-Spectrum Techniques for Bio-Friendly Under Water Acoustic Communication,” *IEEE Access,* vol. 6, pp. 4506-4520, 2017.

[10] M. T. Bin Ali, “Development of Acoustic sensor and signal processing technique,” Ph.D. dissertation, University of Bradford, Bradford,UK, 2010.

[11] Keysight, "Keysight Technologies, Digital Modulation in Communication System-An Introduction," 31 July 2014. [Online]. Available: https://www.keysight.com/gb/en/assets/7018-09093/application-notes/5965-7160.pdf. [Accessed 6 10 2021].

[12] L. C., K. K., F., Bake and L. Enghardt, "Attenuation of sound in wide ducts with flow at elevated pressure and temperature," *Journal of Sound and Vibration,* pp. 3440-3458, 2014.

[13] K.V. Horoshenkov, Y.A. Yin, A. Schellart, R.M. Ashley and J.R. Blanksby, "The acoustic attenuation and hydraulic roughness in a large section sewer pipe with periodical obstacles," Water Science and Technology, Vol. 50 (11), 97–104 (2004).

[14] Y. Yin and K. V. Horoshenkov, "Attenuation of the higher-order cross-sectional modes in a duct with a thin porous layer," J. Acoust. Soc. Am., Vol. 117(2), 528-535 (2005).

Appendix

The supplementary dada can be found via google drive link:

https://drive.google.com/drive/folders/14GEX1krw5hT_oIzl_umDITaDeS-Euqg7?usp=sharing